Geometry and electric power effects on specific impulse and efficiency of an arc-jet thruster

IEPC-2007-232

Presented at the 30th International Electric Propulsion Conference, Florence, Italy
September 17-20, 2007

A. Kaminska* and A. Bialek†
IEPE, Poznan University of Technology, Poznan 60-965, Poland

M. Dudeck‡
ICARE laboratory, Orléans 45071 and University of Paris 6, Paris 75252, France

Abstract: The properties of an argon D.C. arc-jet thruster for space propulsion functioning at low electric power (around 10 kW) and low mass flow (0.5 g/s) are determined. The physical description of the arc takes into account non-equilibrium conditions for local kinetic temperatures and ionization effect. The plasma properties (velocity, pressure, electron and heavy particles temperatures and densities) are calculated by a Navier-Stokes modeling. The influence of different plasma source geometry as angle and length of the nozzle divergent part and electric power on thrust, specific impulse and arc-jet efficiency are discussed.

Nomenclature

$A1$	=	nozzle throat and inlet divergent part cross section
$A2$	=	nozzle outlet cross section
E	=	electric field
F	=	axial thrust
I	=	arc current
I_{sp}	=	specific impulse
j	=	current density
$\dot{m}$	=	gas flow rate
L	=	length of the divergent
n_n	=	heavy particles density
n_e	=	electron density
p	=	total pressure
p_h	=	heavy particles pressure
p_e	=	electron pressure
r	=	radial axis
T	=	heavy particles temperature
T_e	=	electron temperature
u	=	longitudinal component of the flow velocity
v	=	flow velocity

* Professor, Institute of Electric Power Engineering, Aniela.Kaminska@put.poznan.pl
† Assistant, Institute of Electric Power Engineering, Arkadiusz.Bialek@put.poznan.pl
‡ Professor, ICARE laboratory, Michel.Dudeck@cnrs-orleans.fr

U	=	arc voltage
κ_h	=	heavy particles thermal conductivity
κ_e	=	electron thermal conductivity
η	=	global efficiency
σ	=	electric conductivity

I. Introduction

Low power D.C. arc plasma sources working at atmospheric pressure are used for many technological applications. They can also be used for propulsion in space in a large range of power up to 200 kW with a continuous functioning during a few hundreds of hours and with a global efficiency around 50 per cent[1]. Though the technology of arc-jet is now well known, the detailed physical processes involving arc and plasma expansion are not fully understand and described. Although the arc-jets retain today a low interest from the space agencies, the modeling of these plasma sources presents a large benefit for the fundamental researches of supersonic plasma flows with a local thermodynamic non-equilibrium (NLTE) as well as for the thermal processes (T, T_e, T_{vj}) and the chemical processes involving neutral and ionized species. These researches found another application in space for the simulation of the non-equilibrium plasma flows around a spacecraft during the cross of a planetary atmosphere.
We present a numerical determination of physical properties of a D.C. axisymmetric arc-jet running with argon. The set of the local balance equations (species, momentum and electron and heavy species energies) inside the D.C. arc-jet has been previously detailed[2]. Inside an arc, Joule heating of electrons is assuming and non elastic collisions between electrons and neutral atoms of argon produce ions only singly ionized. We assumed electric neutrality (no potential sheath effects, scale of observation greater than Debye length), a law of perfect gas with two temperatures and an axisymmetric and stationary plasma flow without turbulence effects. The global discharge potential in the arc-jet is calculated form the axial electric field (the radial component of the electric field is neglected) witch is deduced from the arc current intensity conservation along the arc-jet axis. Thrust, specific impulse and global efficiency are calculated for different geometry of the divergent part of the arc-jet nozzle.

II. Plasma source

The axisymmetric nozzle of the arc-jet is made of copper and the throat is protected by a tungsten cylinder. This part of nozzle acts as anode. The cathode is a small plane disk set at the nozzle axis near the inlet of the cylindrical throat. The cathode is 2 mm of diameter. The principle construction of the arc-jet has a following geometry dimension. The cylindrical throat is 4 mm of diameter and length. The divergent part of the nozzle is conical with a length of 55 mm and a half angle of 30°. Cathode and anode are cooled by two separated water circuits to perform energy balances of the electrodes. The arc-jet operates with mass flow rate in the range of 0.1 - 0.5 g/s. The electric power supply allows controlling the arc current from 50 to 140 A and total input electric power up to 10 kW with efficiency about of 50%. Plasma plume produced by an arc-jet is shown in Fig. 1.

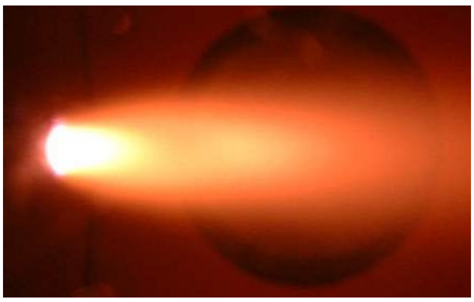

Fig.1. Plasma generated by an arc-jet thruster in the ICARE laboratory test facility

III. Model

The modelled plasma consists of electric arc and plasma jet. Electric arc is generated in the nozzle throat and heats the gas flowing into divergent part of nozzle. We consider that the arc is developed from cathode spot where the current density is high enough to heat the cold gas flowing into nozzle. As is shown[3, 4] the current density in cathode spot with thermo-emission effect is the order of 10^8 A m^{-2}. The Joule's heat corresponding to this current density value and low electric plasma conductivity is the order of 10^{12} W m^{-3} and it is much higher than in the arc column region. The Joule's energy is absorbed by electrons because of plasma electric conductivity created mostly by these particles. Near the cathode the most important parts of this energy is transfer to heavy particles (neutral atoms and ions) in elastic collisions. This effect results from important difference between electron and heavy particles temperatures and high collisions frequency between atoms and electrons. The energy obtained from electrons heats and accelerates the gas. Going away from the cathode the axial gradients of pressure and temperature decrease, the arc column is formed and the important radial gradients near the wall appear causing the heat transfer to the wall. Designer of plasma thrusters must focused attention on cathode flow region of the arc. For arc-jet working with the end of this region at the inlet of divergent part, it is possible to obtain high value of the thrust for minimal energy loss. In the plasma thrusters, the flow can be considered as laminar and continuum. The model of cathode flow region has to take into account two temperatures medium consisting of electrons and heavy particles heaving temperature T_e and T respectively. These temperatures can be determined using energy balance equations written separately for two kinds of particles:

$$\nabla \cdot \left(\frac{5}{2} n_e k T_e v \right) = (v \cdot \nabla) p_e - \kappa_e \nabla T_e - Q_{elas} - Q_{rad} - Q_{ion} + \frac{j^2}{\sigma} \tag{1}$$

$$\nabla \cdot \left(\frac{5}{2} n_h k T_h v \right) = (v \cdot \nabla) p_h - \kappa_h \nabla T_h + Q_{elas} \tag{2}$$

where j^2 / σ is the term representing heat input by Joule effect, j is the current density, σ is electric conductivity taken from[5], Q_{rad} is the radiation loss[6], Q_{elas} is the energy exchange between electrons and heavy particles in elastic collisions, Q_{ion} is atoms ionization energy (or recombination energy), n_e and n_h are electron and heavy particles density respectively, k is the Boltzmann constant, v is flow velocity, p_e and p_h are partially electron and heavy particles pressures and κ_e and κ_h are electron and heavy particles thermal conductivities given by[6] and[7] respectively.
The energy transfer from electrons to heavy particles in the elastic collisions is given by:

$$Q_{elas} = 3 k n_e \frac{m_e}{m_n} (\nu_{ei} + \nu_{en})(T_e - T) \tag{3}$$

where m_e and m_n are the electron and neutral atom masses respectively, ν_{ei} and ν_{en} are the average elastic collision frequencies between electron-ion and electron-neutral:

$$\nu_{ei} = \frac{e^4 n_e \ln \Lambda}{12 \pi \varepsilon_0^2 \sqrt{2 \pi m_e k^3 T_e^3}} \quad \text{and} \quad \nu_{en} = n_n Q_{en} \sqrt{\frac{8 k T_e}{\pi m_e}} \tag{4}$$

where e is the electric charge, ε_0 is the dielectric constant, $\ln\Lambda$ is Coulomb logarithm, Q_{en} is the average electron-neutral collision cross section[8].
We assume that the arc plasma is singly ionized and the ionization process is described by the following three body collision process for the recombination:

$$Ar^+ + e + e \Leftrightarrow Ar + e \tag{5}$$

giving the electron source term S_e written as:

$$S_e = Sn_e(ioniz) - Sn_e(recomb) = k_{ion} n_n n_e - k_{rec} n_e^3 \tag{6}$$

where the ionisation rate k_{rec} is given by[9] and ionisation rate k_{ion} is calculated from the equilibrium relation. The atoms ionization energy (or recombination energy) source term is expressed as:

$$Q_{ion} = S_e E_{ion} \tag{7}$$

where E_{ion} is ionization energy of argon atom.
The conservation equation for electrons is:

$$\nabla \cdot (n_e v) = \nabla \cdot (D_a \nabla n_e) + S_e \tag{8}$$

where D_a is the electron ambipolar diffusion coefficient[7] expressed as a function of (T_e, T).
To calculate other particles density we use the plasma electric neutrality assumption i.e. the electron n_e and ion n_i densities are the same and the equation of state:

$$p = (n_i + n_n)kT + n_e kT_e = p_h + p_e \tag{9}$$

The velocity of flow is determined using the total mass continuity equation

$$\nabla \cdot (\rho v) = 0 \tag{10}$$

and momentum conservation equation

$$\nabla \cdot (\rho v v) = -\nabla p + \nabla \tau \tag{11}$$

where τ is the stress tensor taken into account plasma viscosity determined by[10] and ρ is the mass density defined as:

$$\rho = n_i m_i + n_n m_n + n_e m_e \approx (n_i + n_n) m_n = n_h m_n \tag{12}$$

where m_i is the ion masse and because of small electron mass compared to the ion $m_i \approx m_n$.
The axial electric field is determined considering only longitudinal component

$$E = \frac{I}{2\pi \int_0^{r_c} \sigma r dr} \tag{13}$$

The arc current is kept constant in all the cross section of the throat. Integration of electric field on arc length gives total arc voltage and then the estimation of power input is possible. However we must note that the expression (13) gives good approximation for long arc column when the voltage drops in cathode layer is negligible compared to the arc column voltage.

IV. Physical properties

Firstly, the physical properties at the inlet of nozzle divergent part (or at the throat exit) are presented. Their radial evolutions are shown for different arc currents and theses values are used as inlet boundary conditions to determine the plasma properties in the divergent part of the nozzle. Secondly, for a geometry with a ratio of divergent part cross sections A2(outlet)/A1(inlet) = 100, the radial profiles are shown at the nozzle exit. These calculations are performed for an argon mass flow rate of 0.5 g/s.

IV.1 Plasma properties at the throat exit

The radial distributions of longitudinal component of flow velocity, pressure, heavy particles and electron temperatures, electron and gas densities at the throat exit for a current varying between 60 A and 140 A are presented in Fig. 2. The results of velocity calculation implies that at the throat exit the velocity reaches sonic value what assures supersonic flow in central region of the divergent part. With current increasing, the longitudinal component rises in studied conditions from 1800 m/s to 2600 m/s (Fig. 2a). This effect results from pressure gradients becoming more important for gas heating at higher currents (Fig. 2b). It must be however noted that the value of sonic velocity increase with gas temperature, therefore at the throat exit the Mach numbers is equal to 1 for all current values.
The radial distribution of pressure shows that in central region of the arc and near the wall the pressure is high and its minimum values appear at a distance about 1.6 mm from the throat axis (Fig. 2b). This effect is also slightly present in velocity distribution. It is probably due to the arc column development with hot arc core and ambient cold gas.
The temperatures of heavy particles and electrons increase with the arc current intensity (Fig. 2c and 2d). We note the thermal non equilibrium: the electron temperature is always greater than the heavy particles temperature. However, the deviation from equilibrium condition diminishes with the increase of the current. It can also be seen important radial gradients of heavy particles temperature thus we can predict important heat flux to the wall having effects on arc-jet efficiency. The electron temperature profiles present lower radial gradients and the thermal conductivity of electrons, in study conditions, is much lower than heavy particles therefore the heat electron transfer to the wall is less important than the heavy particles.
The calculated radial electron density profiles (Fig. 2e) correspond to electron temperature profiles as shown in Fig. 2d. Evidently, electron density increases with current rise but heavy particles density in central arc region demonstrates the inverse relation. This implies that the lowering of neutral atoms density resulting of pressure effect is more important than increasing of electron (ion) density.

a)

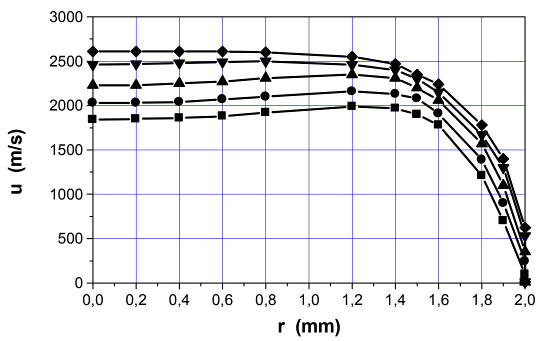

b)

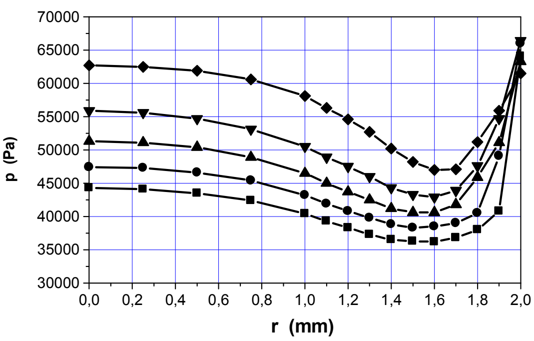

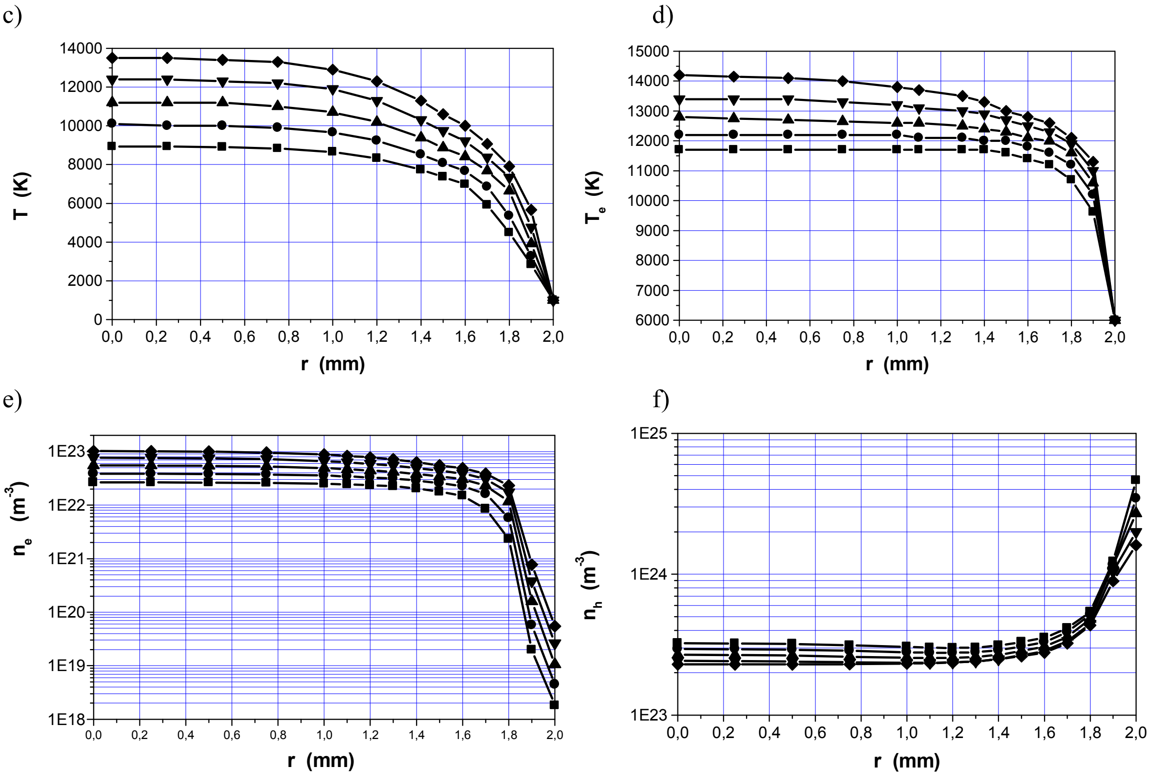

Fig.2. Radial distributions at the throat outlet for a current of —■— 60 A, —●— 80 A, —▲— 100 A, —▼— 120 A, —Λ— 140 A: a) longitudinal flow velocity, b) pressure, c) heavy particles temperature, d) electron temperature, e) electron density, f) heavy particles density

IV.2 Plasma properties at the nozzle exit

As we early mentioned the radial distributions of longitudinal velocity, pressure, heavy particles and electron temperatures and densities are presented (Fig. 3) at the nozzle exit for a current varying between 60 and 140 A and a ratio of cross section A2/A1 =100. The length of nozzle divergent part is 55 mm.
The figure 3a shows the acceleration of the gas in the divergent part with a gain of a factor two compared to the inlet velocity. We can also see that with current increase, the velocity in central region of the jet significantly increases too.

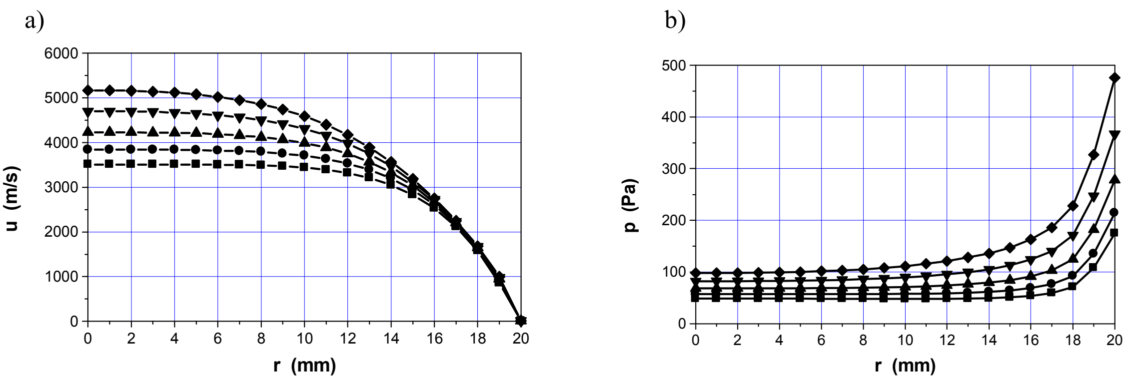

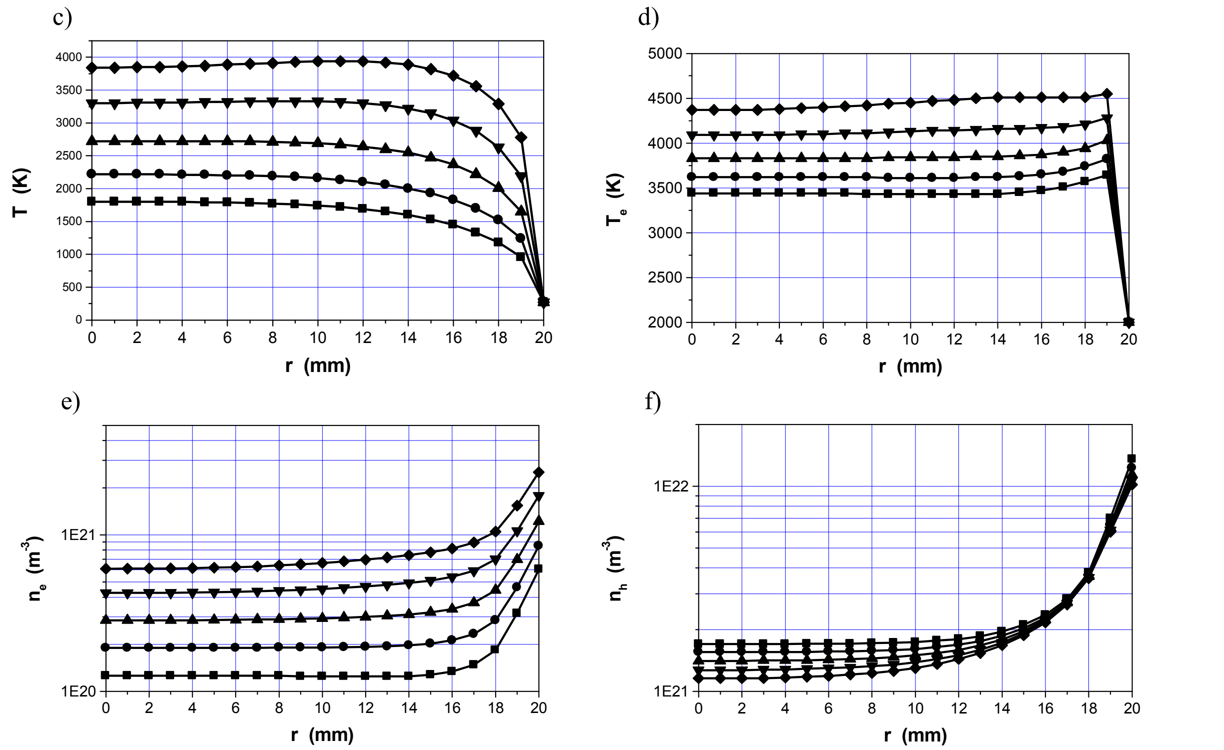

Fig.3. Radial distributions at the nozzle outlet for a current of —■— 60 A, —●— 80 A, —▲— 100 A, —▼— 120 A, —Λ— 140 A: a) longitudinal flow velocity, b) pressure, c) heavy particles temperature, d) electron temperature, e) electron density, f) heavy particles density

The velocity radial profiles imply large dynamic boundary layer, which does not correspond to thermal boundary one. The similar to velocity profile is the profile obtained for heavy particles density (Fig. 3f) although the inverse tendency with a current changing is conserved.

The behavior of the total static pressure (Fig. 3b) shows a large fall of pressure in the central part of the jet (a pressure lower than 100 Pa is obtained whatever the current) and an increase in the wall surface direction. The temperature of heavy particles presents similar behavior at the divergent inlet and outlet evidently with lower levels due to the gas expansion. Because of small thermal conductivity of electrons their temperature profiles become flat, only near wall the temperature adapts to assumed wall condition. It seems that in central flow region with high velocity the electron density results only expansion effect but going to wall direction where the flow velocity decreases the ionization occurs and electron density increases. It would explain the difference between electron temperature and density profiles (Fig. 3d and 3e). A strong fall of particles densities is observed in the divergent: for a current of 140 A, in the divergent the electron density is decreasing from 10^{23} to $6{\cdot}10^{21}$ m^{-3} and neutral atom from to $3{\cdot}10^{23}$ to $1.8{\cdot}10^{21}$ m^{-3} along the nozzle axis.

V. Thrust and efficiency

The axial thrust $F = \int_0^R \rho u^2 2\pi r\, dr$ (R is the radius of nozzle exit section) is calculated for different ratio A2/A1, arc current of 100 A and keeping constant all the other parameters (geometry of throat, length of the nozzle divergent part, argon mass flow rate). The figure 4a presents the axial thrust for A2/A1 varying from 49 to 210. A second series of calculations of the thrust is carry out for different lengths L of the nozzle divergent part and the ratio A2/A1 = 100. The axial thrust for a length of 29, 55 and 84 mm is shown in Fig. 4b.

a) b)

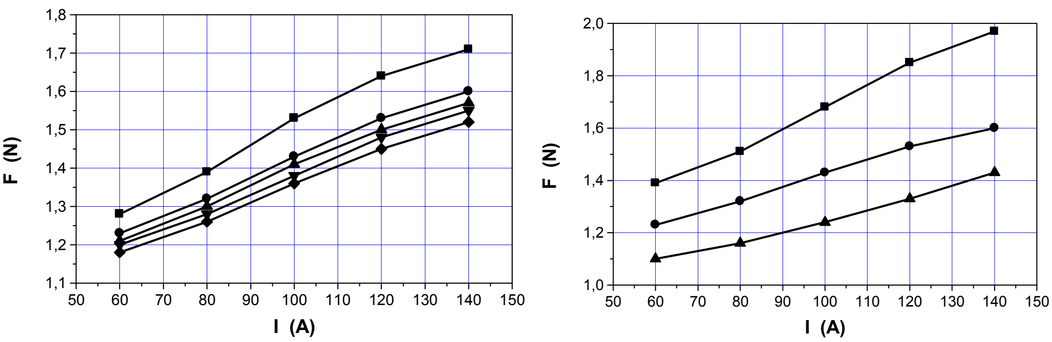

Fig.4. Thrust: a) for the ratio A2/A1 of —Λ— 49, —▼— 64, —▲— 81, —●—100, —■— 210, b) for the nozzle divergent part length of —▲— 29 mm, —●— 55 mm, —■— 84 mm

The specific impulse *Isp* of the arc-jet is defined as $I_{sp} = \dfrac{F}{\dot{m} g_0}$ where $\dot{m}$ is the argon mass flow rate and g_0 is the gravity at the ground level. The specific impulse, calculated for the same conditions as the results presented in figure 4, is shown in Fig. 5. For two studied geometrical conditions of the nozzle divergent part, the specific impulse increases with the arc current. Because of the longitudinal component of the velocity (Fig. 3a) increasing and heavy particles density decreasing (Fig. 3f) with current we can conclude that for considering conditions the effect of velocity behavior is dominant compared to the decrease of the mass density (gas expansion in the divergent part). The figure 4a shows that the specific impulse increases with the ratio A2/A1 that is to say it increases when the angle of the divergent increases for a fixed divergent length. It is the same velocity effect. The specific impulse is varying from 240 to 350 s. The effect of the divergent part length on specific impulse is demonstrated in Fig. 4b. This is not surprising because the results are obtained for the same outlet cross section of the nozzle. Therefore, for longer divergent part the angle is smaller and at the nozzle exit the plasma density is higher. The specific impulse is then varying between 220 and 400 s.

a) b)

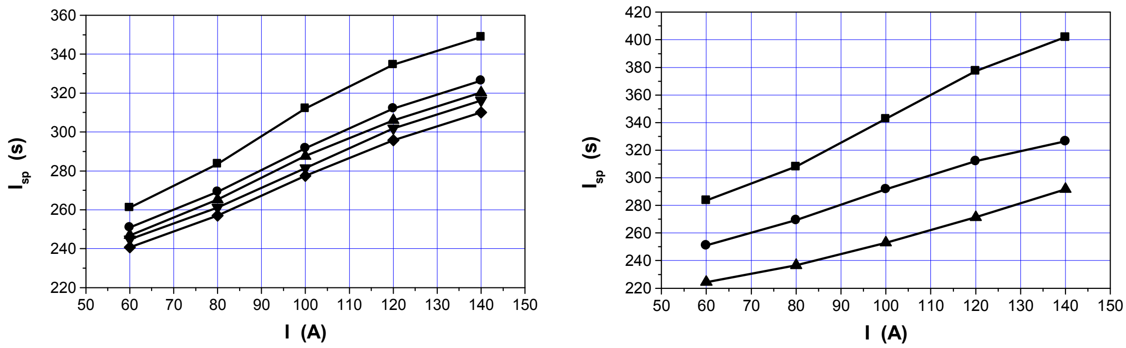

Fig.5. Specific impulse for: a) the ratio A2/A1 of —Λ— 49, —▼— 64, —▲— 81, —●—100, —■— 210, b) the nozzle divergent part length of —▲— 29 mm, —●— 55 mm, —■— 84 mm

The calculation of the efficiency of the arc-jet thruster requires the voltage determination which is obtained from the longitudinal component of the electric field given by Eq. 13. The input electric power is then deduced as a function of the arc current (Fig. 6).

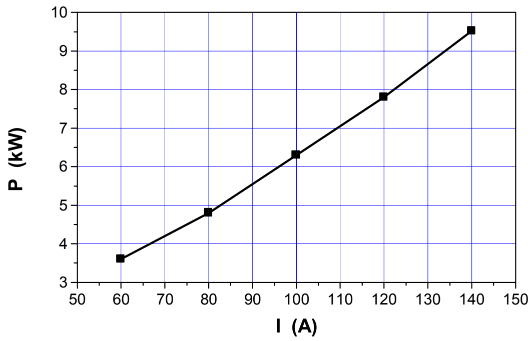

Fig.6. Electric power as a function of arc current

The global efficiency is defined by: $\eta = \dfrac{F^2}{2\dot{m}\,I\,U}$. For the studied geometrical divergent part conditions (for ratio A2/A1 and for the length of the divergent part), this efficiency presents a quasi linear decrease with the arc current. It is not surprising, because of the energy loss to the wall increase with arc current. The same effect explains the efficiency decreasing for smaller angle and longer nozzle divergent part.

a) b)

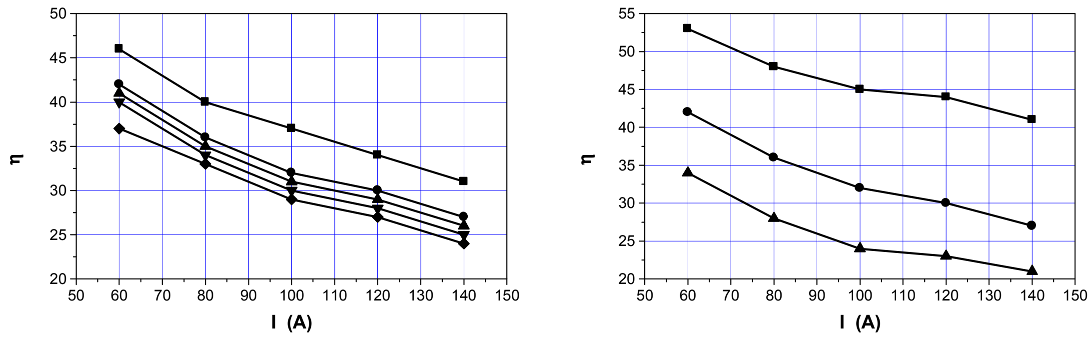

Fig.7. Efficiency as current function for: a) the ratio A2/A1 of —Λ— 49, —▼— 64, —▲— 81, —●—100, —■— 210, b) the nozzle divergent part length of —▲— 29 mm, —●— 55 mm, —■— 84 mm

VI. Conclusion

A two-temperature fluid description permits to calculate all the physical properties of a D.C. arc-jet taking into account a non equilibrium condition for the argon ionization process and for the two kinetic temperatures. The specific impulse and the global efficiency are calculated for two variations of the geometry of the nozzle divergent part: firstly the ratio between the cross sections at the nozzle outlet and inlet is changed for a fixed length, secondly this cross section ratio is fixed and the length of the divergent part changes. For the studied conditions of mass flow rate (0.5 g/s) and for the range of arc current (60-140 A), the calculated thrust is between 1.1 and 2 N, the specific impulse varies from 220 to 400 s and the arc jet efficiency from 0.21 to 0.53. It has been shown that the thrust and the specific impulse increase with the arc current especially because of flow acceleration. However, for higher currents the energy loss to the wall becomes more and more important and the efficiency of arc-jet thruster diminishes. The similar effect is observed for longer divergent part and smaller divergence angle. The presented study allows concluding that design of arc-jet requires calculation permitting optimizing this kind of plasma sources.

References

[1]Wallner, L. E., Czika, J. Jr., "Arc-jet thrustor for space propulsion," NASA TN D-2868, 1965.

[2]Kaminska, A., Barbosa, E., Lopez, B., Izrar, B., Dudeck, M., "Modeling of an argon plasma jet generated by dc arc", *Plasma Sources Sci. Technol.*, submitted.

[3]Rethfeld, B., Wendelstorf, J., Klein, T., Simon, G., "A self-consistent model for the cathode fall region of an electric arc," *J. Phys. D: Appl. Phys.,* 29. 1996, pp. 121-128.

[4]Roth, J. R., *Industrial Plasma Engineering - Vol. 1: Principles*, Inst. Physics Publishing, Bristol and Philadelphia, 1995.

[5]Devoto, R. S., "Transport Coefficients of Ionized Argon," *Physics of Fluids*. Vol. 16. No. 5, 1973, pp. 616-623.

[6]Kroessen, G. M. W., Shram, D. C., Timmermans, C. J., De Haas, J. C. M., "The Energy Balance of a Plasma in Partial Local Thermodynamic Equilibrium," *IEEE Trans. Plasma. Sci.*, Vol. 18, No. 6, 1990, pp. 985-991.

[7]Devoto, R. S., "Transport coefficients of partially ionized argon," *Physic Fluids.*, No. 10, 1967, pp. 354-364.

[8]Milloy, H. B., Crompton, R. W., Rees, J. A., Robertson, A. G., "The Momentum Transfer Cross Sections for Electrons in Argon in the Energy Range 0–4 eV," *Austr. J. Phys.,* Vol. 30, No. 1, 1977, pp. 61-72.

[9]Hoffert, M. I., Lien, H., "Quasi-One-Dimensional, Nonequilibrium Gas Dynamics of Partially Ionized Two-Temperature Argon," *Physics of Fluids*, Vol. 10, No. 8, 1967, pp. 1769-1777.

[11]Blottner, F. G., Johnson, M., Ellis, H., Sandia Natl. Laboratories, SC-RR-70-754, 1971.